CONCRETE LIBRARY OF JSCE NO. 19, JUNE 1992

IMAGE ANALYSIS OF AIR-VOID SYSTEM IN HARDENED CONCRETE

(Translation from Proceedings of JSCE,.No. 420/V-13, Aug. 1990)

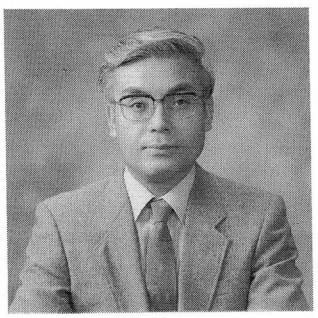

Koichi AYUTA

Hiroshi SAKURAI

Kan-ichiro TANABE

SYNOPSIS

The standard microscopic technique for the characterization of air-voids in hardened concrete accords with ASTM C457, but is a time-consuming process requiring much effort. Recently, a technique based on an image analyzing system has been developed in order to eliminate these difficulties. However, the specimens analyzed by this system have to be given a surface treatment to make visible the air-voids in the cement paste matrix. This paper describes the operation of the new automatic quantitative image analyzing system which measures difference in intensity of reflected illumination from non-treated specimens. The surface of a specimen is illuminated from three directions. The time required to measure the air-void system of a 10 cm-square specimen is approximately one hour.

K. Ayuta is a professor at Department of Civil Engineering of Kitami Institute of Technology, Kitami, Hokkaido, Japan. He received his doctorate in engineering from Hokkaido University in 1983. His research interests include the durability of concrete structures in cold regions, cold weather concreting and marine concrete. He is a member of JSCE, JCI and ACI.

H. Sakurai is an assistant professor at Department of Developmental Engineering of Kitami Institute of Technology, Kitami, Hokkaido, Japan. He received his doctorate in engineering from Hokkaido University in 1992. His research has been on prediction and evaluation of service year of concrete structures in cold regions. He is a member of JSCE, JCI and ACI.

K. Tanabe is a chief engineer at Nireco Corporation,. Tokyo, Japan. He graduated from Kohgakuin Institute of Technology in 1975. His research interests include the image analyzing system.

---

1. FOREWORD

In order to ensure a concrete structure's durability against frost damage, an appropriate amount of air must be entrained into the concrete. Quality control is achieved by measuring the amount of air in the fresh concrete. However, in order to evaluate durability against frost damage, the spatial distribution of air voids is more critical than actual amount of air. Thus, characterization of the air voids in hardened concrete is necessary.

The standard techniques for measuring the characteristics of the air-void system in hardened concrete are the point-count method or the linear-traverse method in accordance with ASTM C457. However, since such methods require observations and measurements under a microscope, they consume significant amounts of time and effort.

Recently, an image analyzing system has been developed to eliminate these difficulties [1]-[5]. An image is captured by a TV camera, and then fed into a computer for analysis. This system significantly reduces the time and effort required for measurement compared with the ASTM methods. However, it is difficult for the system to directly distinguish air voids in the hardened concrete using the image obtained by a TV camera. Prior processing of the sample is required to distinguish air voids from other areas. Several techniques are utilized to make the air voids more easily distinguishable. In one technique, the air voids on the surface of the hardened concrete are filled with white solvent and the rest of the surface is tinted black; in another, the air voids are filled with a material fortified with fluorescent paint and exposed to ultraviolet light. When such processing is considered, even though the time required for the measurement is reduced by using image analysis, the actual total time require for testing is not reduced at all.

Given this situation, the authors attempted the image analysis of hardened concrete samples without prior processing, and successfully developed a technique which enables the air voids in hardened concrete to be measured rapidly.

2. OUTLINE OF THE IMAGE-ANALYZING SYSTEM

This image analysis system consists of an image processing device, a macroscopic input device that feeds in the image data needed to distinguish aggregate areas and cement paste areas, a microscopic input device that feeds in image data from a microscope to distinguish the air voids, and a printer that makes hard copies of the data.

Figure 1 is a block diagram of the image analysis system.
"1" is the concrete sample being measured.
"2" is a vibration-free table to eliminate vibrations of the sample.
"3" is an XY stage for moving the sample in two dimensions on the table.
"4" is the controller for the XY stage.
"5" is an automatic focusing stage that adjusts the distance for best focus.
"6" is a focus control that controls automatic focusing stage "5".
"7" is the microscopic camera used to distinguish air voids in sample "1".
"8" is the macroscopic camera used to distinguish between aggregate areas and cement paste areas in sample "1".

"9" is the camera control equipment for camera "7" and camera "8".
"10" is a camera selector which switch on/off cameras "7" and "8".
"11" is the lighting equipment for illuminating sample "1" with three lights; from the top, the right, and the left sides.
"12" is the image-processor that operates on images fed from cameras "7" and "8", and controls the XY stage controller "4", the automatic focus controller "6", and the camera selector "10".
"13" is a personal computer that controls the image-processor "12".
"14" is a secondary storage device consisting of a microdisk and floppy disks holding programs for the personal computer "13" and measurement data deriving from the image-processor "12".
"15" is a printer for measurements and other data from image processor "12".

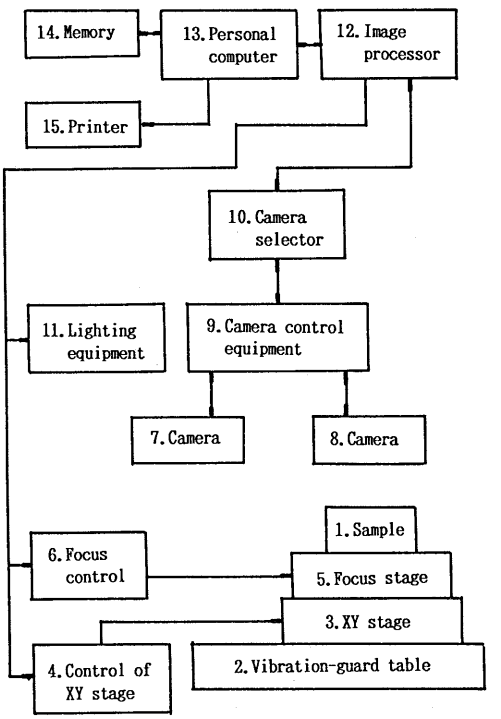

Note; 7: Air-void system camera
8: Camera to distinguish between hardened cement paste and aggregate

Fig. 1 Block diagram of the image analyzing system.

The input unit is shown in Photo 1, and the lighting equipment for microscopic measurements in Photo 2.

3. AIR VOID RECOGNITION PROCESS

The image from the TV camera is converted into a video signal pixel by pixel, with the shades of bright and dark progressing from 0 for black to 255 for white. These signal strengths are then digitized. A cut-off value is set

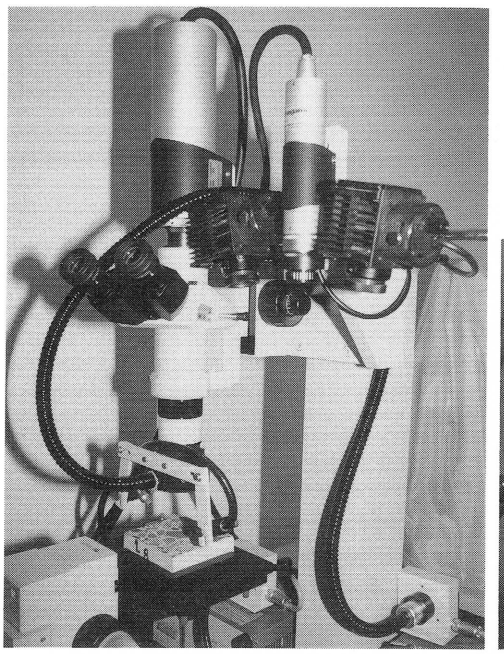

Photo 1 An input unit.

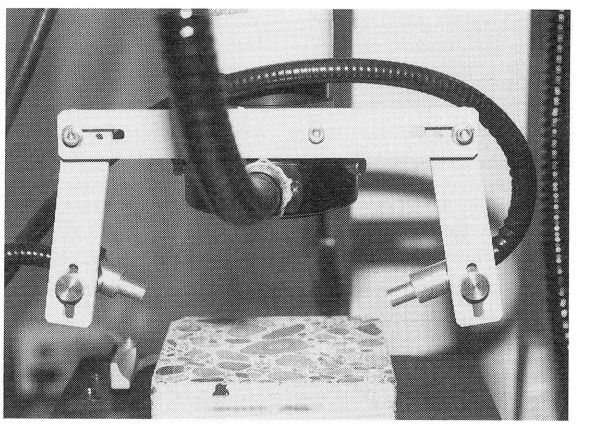

Photo 2 Lighting equipment

among these 256 shades, and a pixel above the particular value is converted to 1, and one below it is converted to 0 to form binary data.

In this study, the top, right, and left sides of the sample were exposed to a uniform strong light. An image was taken of the surface under each illumination angle and the differences in reflected light levels at the same location measured, thus clarifying the location of air voids. That is to say, when the surface of the sample is illuminated from different directions, the level of reflected light from the air voids is different.

Figure 2 is a drawing which shows the sample surface exposed to even light from the top, the left, and the right. Figure 2(a) shows the shape of one air void and the direction of the illumination. Figure 2(b) shows the distribution of reflected light and shade formation when exposed to overhead light. Reflected light levels are described in increments from 0 to 255. Light from air void areas is represented by *"ol"* and from other areas by "*OL*". Light distribution and shade formation are shown in Fig. 2(c) when the sample is exposed to light from the right, and in 2(d) when exposed to light from the left. "*rl*", "*RL*", "*ll*", and "*LL*" represent reflected light levels at the same location as the respective points in Fig. 2(b). Comparing 2(b), 2(c), and 2(d), the reflected light levels in areas other than where there are air voids, namely "*OL*" "*RL*", and "*LL*", are the same, but the levels in air-void areas at the same points differ according to the direction of the light. This difference allows air voids to be detected.

The air voids were detected as follows: Reflected light measurements when exposed to light from three directions, "*ol*", "*rl*", and "*ll*", were taken on three-dimensional coordinates as shown in Fig. 3. A vector from the origin

(0,0,0), [*ol*, *rl*, *ll*] crosses a triangular plane [1, 1, 1], with vertexes (1, 0, 0), (0, 1, 0), and (0, 0, 1) at point S.

A vector [1, 1, 1] whose three coordinates with the same value from the origin of the coordinate O crosses plane [1, 1, 1] at a point which is defined as the origin O' of a reflectance-coordinate system (Fig. 4).

A vector from the origin O' to point S allows an air void to be detected by size. The greater the vector, the more likely that it is an air void.

The size of vector *V* can be obtained from "*ol*", "*rl*", and "*ll*", the reflected levels at each point exposed to light from the three directions, using the following formula [6].

$$V = C\sqrt{X^2 + Y^2}$$

$$X = \frac{ol - 0.5(rl + ll)}{ol + rl + ll} \qquad Y = \frac{\sqrt{3}(rl - ll)}{2(ol + rl + ll)}$$

C: a constant

In this formula, the coefficient of reflection from the image is a constant. If the vector *V* is greater than the criterion for the existence of an air void in the reflectance-coordinate system, the area is recognized as an air void.

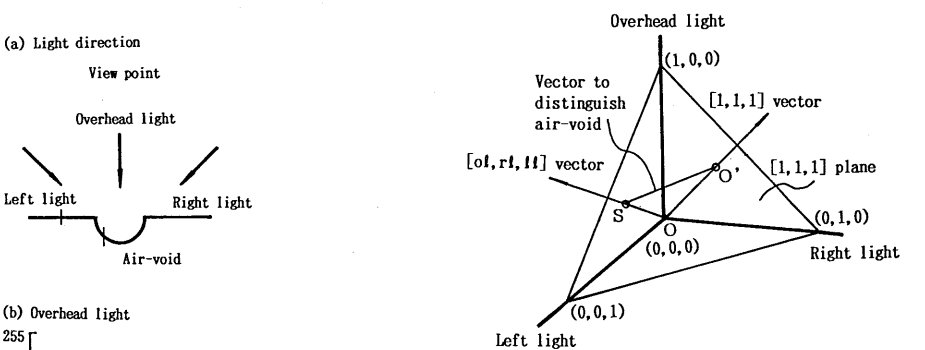

Fig. 3 Vector to distinguish air void.

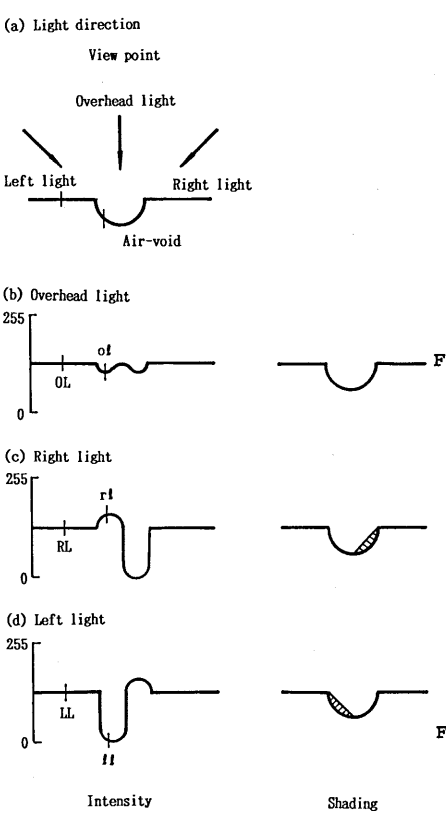

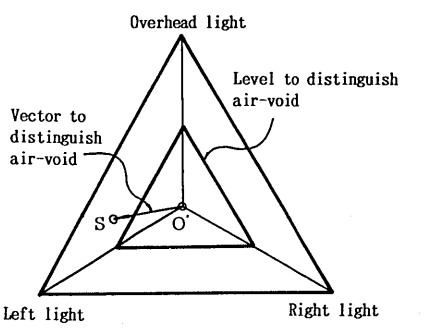

Fig. 4 Plane to distinguish air void.

Fig. 2 Shading from three directions.

4. PROCESSING TO REDUCE MEASUREMENT TIME

Measurements in this image analysis system are in two parts: microscopic measurements, as described in section 3, to distinguish air-void areas in a magnified partial image of the cut surface of a sample; and macroscopic measurements to distinguish cement paste areas and aggregate areas over the entire cut surface of the sample.

In order to distinguish very small air voids in hardened concrete, the optical range for microscopic measurements must be under 10 mm. Several hundred images must be used to obtain accurate characteristics of the air-void system. This process is the most time-consuming of the measurement process. It is desirable to avoid taking images of all-aggregate areas in order to reduce the measurement time. Therefore, macroscopic measurements are used first to determine all-aggregate areas. Microscopic measurements are not then performed on these areas. The origins for macroscopic and microscopic measurements were made coincident by an auto-staging control. In addition, all movements of the sample between macroscopic measurements and microscopic measurements; and all movement during microscopic measurements were carried out automatically to reduce time and labor.

Macroscopic measurements to distinguish between cement paste areas and aggregate areas on the sample section are done by setting a criterion which appropriately recognizes likely aggregate (aggregate areas) from other areas (cement paste areas) through the light and shade distribution in the image data. Figure 5 shows a typical criterion line across a sample section. Above the set criterion are aggregate areas, and below it cement paste areas. However, since this judgment is made according to the light and shade in the image, white-colored aggregates is difficult to recognize. The operator must manually correct the coordinates for white aggregate areas while observing the image on the display. An input device (a mouse) is used for precise discrimination.

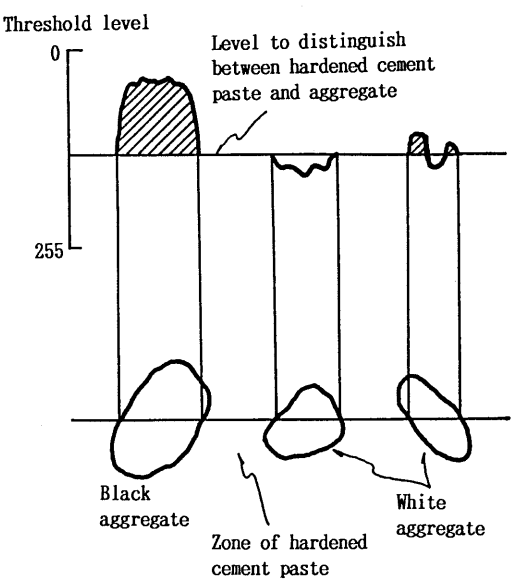

Fig. 5 Distinction between hardened cement paste and aggregate.

5. MEASUREMENT EXAMPLE

The concrete sample used for measurement was 10 cm square. The optical range for macroscopic measurements was 9x9 cm, and the optical range for microscopic measurements was 6x6 mm. There were a total of 225 microscopic optical fields. In this example, the total number of pixels per optical field was chosen to be 400x400. Therefore, one pixel is 15 μm. The standard size of entrained air voids is 50-500 μm. Thus, data for square air voids larger than 50 μm in diameter were input.

Photo 3 shows the binary-digitized image of the sample concrete section as input from the macroscopic camera, showing the distinction between cement paste areas and aggregate areas.

Photos 4-6 show images of a single optical field input from the microscopic camera with overhead, right, and left illumination, respectively.

Photo 7 shows the binary-digitized image derived from Photos 4-6, showing the air voids.

Table 1 shows the measurements of the air-void system. (1) is calculated by the ASTM linear traverse method and (2) is calculated by the ASTM modified point-count method as given by image analysis. Cement paste content is obtained from the binary-digitized image in both methods. For comparison, (3) is the result of an ASTM modified point-count method without image analysis. In this case, the cement paste content is obtained from the mix proportion. The air content in the fresh concrete was 4.6%.

Figure 6 shows the distribution of air-void size obtained from the image analysis. Judging from Table 1 and Fig. 6, it can be concluded that the air-void system of hardened concrete obtained using this image analysis system is highly reliable.

The time required to take the measurements was approximately one hour in both cases (1) and (2). Of this, the operator was only needed for 20 minutes. The operator sets a criterion for the digitizing, and the microscopic measurements are then totally automatic. It would take at least several hours to measure a sample of the same size by the ASTM method. Therefore, the technique described in this paper is significantly effective in saving time.

In addition, since this technique is based on the detection of surface uneveness, it may also be effective for the measurement of cracks in concrete.

Table 1 Results of analysis

	(1)	(2)	(3)
Paste Content (%)	26.6	26.6	26.8
Air-Void Content (%)	3.9	4.0	4.7
Specific Surface (cm^2/cm^3)	256	255	237
Spacing Factor (μm)	209	208	207

(1) Image Analysis based on the Linear Traverse Method of ASTM

(2) Image Analysis based on the Modified Point-Count Method of ASTM

(3) Modified Point-Count Method of ASTM

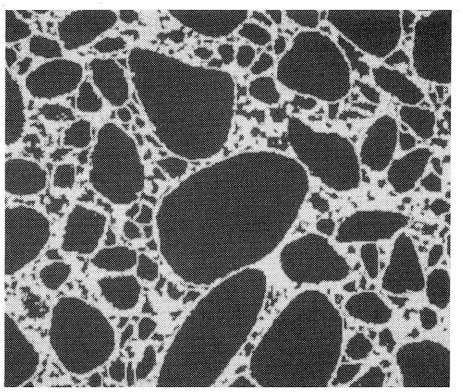

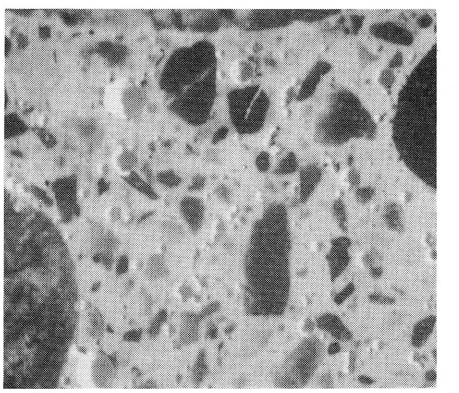

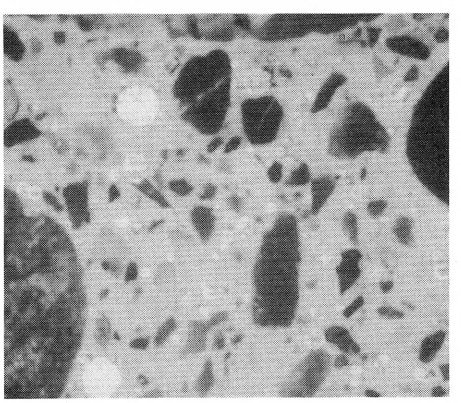

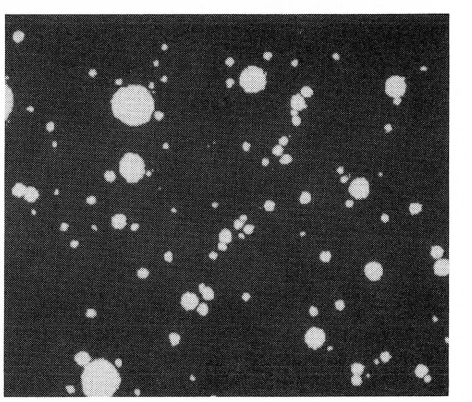

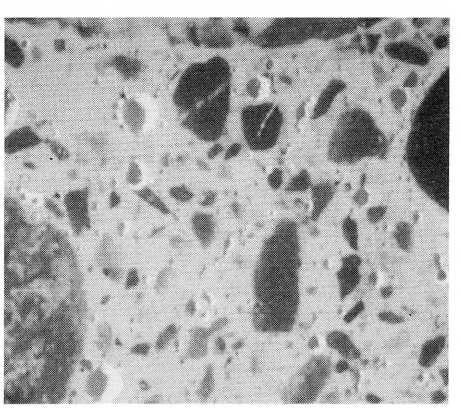

(Left, top to bottom)
Photo 3 Image of concrete section.
Photo 4 Image with overhead light source.
Photo 5 Image with left light source.

(Right, from the top)
Photo 6 Image with right light source.
Photo 7 Image of air-void system.

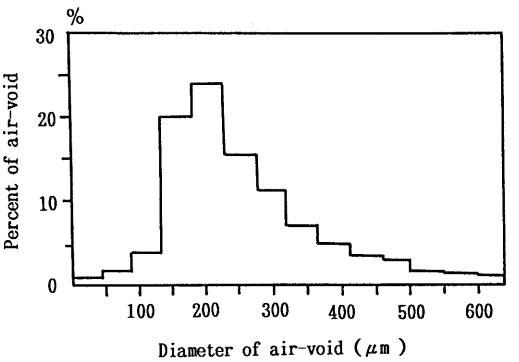

Fig. 6 Distribution of air voids

6. CONCLUSION

Conventional techniques for the characterization of air-void system in hardened concrete require prior processing in order to distinguish air voids from other areas. A new technique is introduced here in which the concrete sample is exposed to light from three directions and air voids are distinguished by differences in reflected light levels, thus eliminating the time-consuming processes. As a result, the rapid measurement of air voids in hardened concrete has become possible without any special processing in advance. The time required to measure a hardened concrete section 10 cm square is only one hour. The operator is only required for 20 minutes of this time because of the automatization of measurements.

ACKNOWLEDGMENTS

The authors gratefully acknowledge the cooperation of Mr. H. Igari and Mr. Y. Takahashi in developing this technique.

REFERENCES

[1] Chatterji, S. and Gudmundsson, H: Characterization of Entrained Air Bubble System in Concrete by Means of Image Analyzing Microscope, Cement and Concrete Research, Vol. 7, No. 4., pp. 423-428, 1977.

[2] Harada, K. et al.: Method of Measurement of Air-void System in Hardened Concrete Using an Image Analyzer, Cement and Concrete, No. 471, pp. 22-28, 1986.(in Japanese)

[3] Ohta, T. et al.: Measurement of Air Void Parameters in Hardened Concrete Using Automatic Image Analyzing System, The Japan Concrete Institute 8th Conference, pp. 389-392, 1986. (in Japanese)

[4] Ayuta, K. and Hayashi, M.: Air Content Recommended for Frost Resistance of Concrete in Sea Water, The Japan Concrete Institute 8th Conference, pp. 93-96, 1986. (in Japanese)

[5] Nishiyama, T. et al.: Staining and Observation of Air-void Systems in Hardened Concrete Using Cyanoacrylate, CAJ Review of the 42nd General Meeting, pp. 170-171, 1988.

[6] Horn, B. and Brooks, M.J.: Shape from Shading, MIT Press, pp. 29-52, 1989.